Waste photopolymer printing matrices as a potential filler of polymeric materials

Krzysztof Moraczewski[1*], Tomasz Karasiewicz[1], Bartłomiej Jagodziński[1],
Andrzej Trafarski[1] , Magdalena Zaborowska[2]

[1] Faculty of Materials Engineering, Kazimierz Wielki University, ul. Chodkiewicza 30, 85-064 Bydgoszcz, Poland
[2] Blue System Sp. z o.o., ul. Rynkowska 17D, 85-503 Bydgoszcz, Poland
* Corresponding author's e-mail: kmm@ukw.edu.pl

ABSTRACT

This study investigated the potential use of waste photopolymer printing matrices as fillers in polymeric materials. Ground printing matrices were incorporated into polypropylene at concentrations of 10, 20, and 30 wt.% and evaluated for selected physical, mechanical, and thermal properties. A spectroscopic analysis indicated that the matrices consist of polyesters and styrene–butadiene copolymer. The resulting composites maintained low density (<1 g/cm³), compared to 0.896 g/cm³ for neat polypropylene. Contrary to most literature reports, the addition of ground printing matrices led to a reduction in mechanical performance. At the highest filler content, tensile strength decreased by 50% (from 22.7 to 10.9 MPa), Young's modulus by 33% (from 1290 to 825 MPa), and flexural strength by 38% (from 37 to 23 MPa). The most pronounced decrease was observed in impact strength, which dropped by 67% to 17 kJ/m². Thermal properties were affected to a lesser extent. The filler slightly reduced the crystallization temperature but simultaneously improved the thermal stability of the composites, with higher filler loading yielding greater enhancement. The observed reduction in material properties is primarily attributed to poor matrix–filler adhesion, representing a key challenge for further development. Nevertheless, the performance remains acceptable for the intended applications. Overall, the study successfully demonstrates the feasibility of using post-production label waste as a polymer filler.

Keywords: polypropylene, printing matrices, polymer waste, recycling, circular economy.

INTRODUCTION

The waste from production processes, including the waste material from printing industry, is a significant problem for companies. Very often, specialized disposal of such waste is necessary, which, given the large production volume, is associated with high costs for enterprises. Additionally, the waste disposal processes themselves, which largely involve pyrolysis, pose a heavy burden on the natural environment, even when modern disposal methods are used. Therefore, recently, great emphasis has been placed on promoting and applying the behavior consistent with the assumptions of circular economy [1–3].

The circular economy (CE) constitutes a regenerative model of economic development, in which the consumption of primary raw materials, the generation of waste, as well as emissions and energy losses are minimized through the establishment of closed-loop processes. Within this framework, by-products and waste streams from certain operations are reintroduced as inputs into others, thereby ensuring the highest possible reduction in overall waste generation. This model is the opposite of a linear economy, based on continuous growth and increasing consumption of raw materials and the volume of waste. In the circular economy model, the aim is to maintain the value of resources for as long as possible (and not to create added value as in the linear economy model), to optimize resource management (and not to optimize resource flows) and to increase the efficiency of the use of goods (and not the

efficiency of goods production) [4]. It should be noted that the transition to the circular economy model is the official goal of the European Union [5], so its implementation is crucial for the companies operating in Europe.

The printing industry represents a sector focused on the manufacture of printed materials. This domain encompasses various printing techniques, including offset printing, digital printing, screen printing, and large-format printing. As with other industrial sectors, printing processes are associated with the generation of waste. Significant forms of solid, liquid, and gaseous waste arise before, during, and after the printing process. These include waste inks, residual ink and solvents from machine cleaning, wastewater from water-based inks, plate and film developer and fixer solutions, waste paper, waste film, defective prints, cleaning solvents, and emissions of volatile organic compounds (VOCs) resulting from the use of isopropyl alcohol (IPA), as well as used printing matrices composed of diverse materials, such as metals and polymers [6–10].

In the modern printing industry, one of the most popular materials used for the production of printing matrices is photopolymers. Photopolymer printing matrices most often consist of four main components/layers [11]. The first layer, most often made of polyester or polystyrene foils, serves as protection against dirt and is removed before the process of creating the actual printing matrix. The second layer, also having a protective function, is most often made of polyamide copolymers or vinyl acetate copolymers. This layer can also be removed in the process of producing the actual polymer matrix, but this requires the use of appropriate solvents. The third layer is the curable layer, which is the main element of the photopolymer printing matrix. This layer consists of a photosensitive elastomeric composition comprising: a layer of a thermoplastic elastomeric block copolymer, e.g., a styrene/butadiene copolymer, and polymerization initiators that can be activated by exposure to light of the appropriate wavelength. The fourth and last layer is the supporting layer, usually made of polyesters.

Only a small number of articles presenting the use of used photopolymer printing matrices can be found in the literature. Cordeiro et al. [12] used waste photopolymer matrices to improve the properties of polypropylene (PP) and ethylene-vinyl acetate (EVA). In their research, they introduced up to 15 wt.% of ground matrix

waste consisting of butadiene-styrene copolymer and polyester with a particle size smaller than 24 mesh (0.5 mm) into the polymer matrix by extrusion. The tests carried out showed that the addition of ground particles of printing matrices did not significantly affect the mechanical properties of the obtained composites. However, their thermal resistance improved, as the recorded degradation temperatures were slightly higher. However, no changes were observed in the chemical structure of the produced composites.

Gürler et al. [13] used polymer matrices in amounts up to 30 wt.% to modify the biodegradable polymer – polycaprolactone (PCL) – in order to use the obtained materials in the packaging industry. New materials were produced by solution casting. The conducted tests revealed that the thermal stability of the obtained materials decreased with increasing filler content. It was also observed that higher filler loadings increasingly restricted the mobility of polymer chains, resulting in an elevated glass transition temperature of the pure PCL matrix. The films containing filler particles exhibited greater opacity compared to pure PCL films. Additionally, the incorporation of filler was associated with enhanced barrier properties against water vapor. However, the study did not report the mechanical performance of the prepared materials.

Kök et al. [14] used waste photopolymer printing matrices to modify bitumen. The functional properties of asphalt modified with photopolymer printing matrices were compared with pure asphalt and styrene-butadiene-styrene (SBS) modification. It was found that the materials containing waste matrices had better properties in terms of higher softening temperature, viscosity, storage modulus and lower phase angle value compared to pure bitumen. The modified waste exhibited greater flexibility than SBS at low temperatures and demonstrated slightly enhanced storage stability.

Ferretto et al. [15] used the remains of photopolymer plates (rubber microparticles) to modify a thermosetting epoxy polymer consisting of bisphenol A diglycidyl ether and triethylenetetramine (DGEBA/TETA). New materials were produced by pouring. The filler planned for use was prepared in two ways. In the first method, used photopolymer plates were shredded and then classified according to particle size. In the second method, polyester layers were separated from used photopolymer plates, and then the remaining

elastomeric fraction was ground by cryogenic grinding. The fillers obtained using this method were incorporated into the polymer matrix at concentrations of up to 7.5 wt.%. The results demonstrated that the filler prepared using the first method was ineffective as a modifier of the epoxy system, as evidenced by a reduction in mechanical properties, including maximum tensile strength and elongation, regardless of filler concentration. In contrast, the filler prepared using the second method led to improvements in tensile strength, deformation capacity, and impact resistance.

Zimmermann et al. [16] examined the effect of introducing photopolymer plate remnants from the flexographic process into polyester-glass composites. The composites were prepared by hand lamination with different waste contents (0, 2.5, 5 and 10 wt.%). The results indicated that the incorporation of spent matrix particles increased lamination difficulty and promoted the formation of larger voids at higher filler contents. While the filler reduced impact resistance, it did not diminish flexural strength or storage modulus, suggesting that, despite the elastomeric nature of the material, the photopolymer plate residue acted predominantly as a reinforcing, rather than a toughening agent.

In their previous work, the authors presented the possibility of using another type of waste from the printing industry, i.e. waste from the label production process, as a filler for polymeric materials [17]. This research aimed to determine the feasibility of utilizing another significant waste material of the printing industry, namely the used photopolymer printing matrices. The element that distinguishes the presented research from prior works found in the literature is the deliberate use of the simplest possible technological operations for both filler preparation and composite production, ensuring a direct path toward industrial scalability. The methodology was intentionally minimalistic, involving only ambient-temperature mechanical shredding of the waste material followed by its incorporation into a polypropylene matrix via conventional melt-processing techniques, such as single-screw extrusion and injection molding. By avoiding such specialized, costly, or non-scalable operations, the current study prioritized a low-cost and accessible recycling pathway, thereby enhancing the feasibility of its adoption by industry for the valorization of post-production printing waste. This will simplify the production of new polymer composites, potentially increasing their output and reducing the waste from unused printing matrices. Additionally, selected physical, mechanical and thermal properties of the obtained composites were examined to determine how the addition of ground matrices would affect the characteristics of the obtained composites and to assess whether the obtained properties would enable their possible use.

MATERIALS AND METHODOLOGY

Materials

Polypropylene (PP) Moplen EP548U (LyondellBasell, the Netherlands) was chosen as the matrix for the new polymer composites. This polymer is characterized by (according to the safety data sheet): density 0.90 g/cm^3, mass flow rate 70 g/10 min (230 °C/2.16 kg), tensile strength 28 MPa, elongation at break 30%, impact strength (notched) 4 kJ/m^2 and Young's modulus 1450 MPa.

The PP matrix was filled with used photopolymer printing matrices. The matrices were industrial waste from the printing process carried out at the Blue System Sp z o. o., (Bydgoszcz, Poland) printing house. The input material was a mixture of printing matrices from various manufacturers and/or distributors from a wide period of the printing house's activity. Therefore, the exact composition of the photopolymer printing matrices used cannot be clearly determined. Therefore, as part of the research, an analysis of the composition of the matrices was carried out, the results of which are presented later in the article.

Before being introduced into the polymer matrix, used photopolymer printing matrices were shredded using a laboratory grinder for polymer materials. The final form of shredded matrices is shown in Figure 1.

Methodology

The shredded waste material of photopolymer printing matrices was incorporated into polypropylene through the extrusion process. Extrusion was performed using a W25-30D single-screw extruder (Metalchem, Poland). To achieve precise homogenization of the filler within the polymer matrix, an intensive mixing screw equipped with additional kneading and reverse segments was employed. The screw rotation speed was
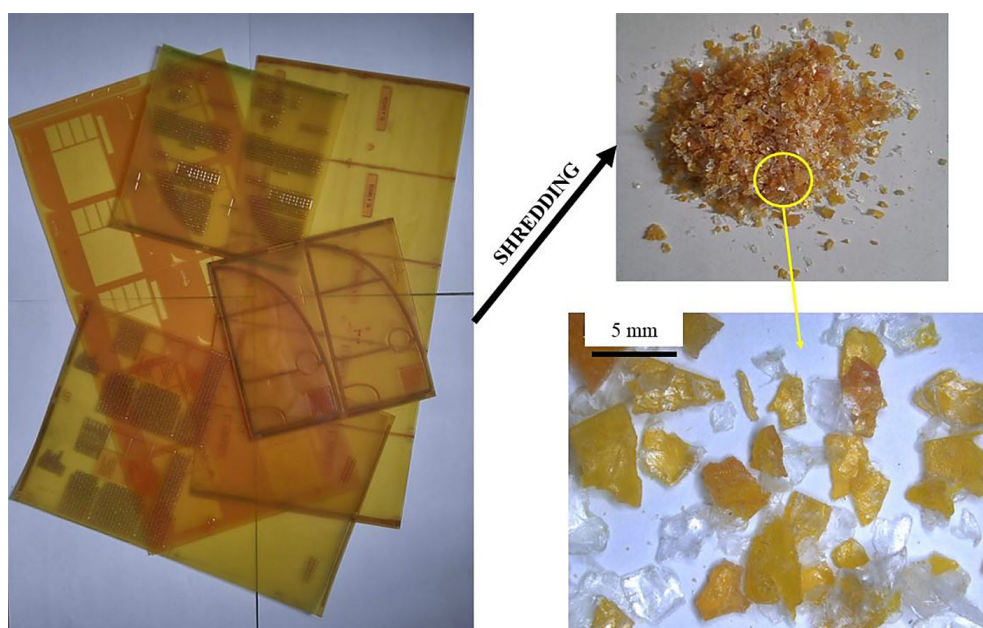
Figure 1. Waste photopolymer printing matrices before and after the shredding process

maintained at a constant 200 rpm. The temperatures of the individual extruder zones were set to 175, 185, 195, and 195 °C, while the extrusion head temperature was maintained at 195°C. The extrudate was subsequently cooled in a water bath and pelletized using a knife granulator. Three composite formulations were prepared, containing 10, 20, or 30 wt.% of shredded printing matrices, designated as P10, P20, and P30, respectively (the numerical designation indicates the filler content). The properties of these composites were compared with those of neat polypropylene (sample P).

Test specimens, in the form of standardized paddles, were produced from the granulate via injection molding (Figure 2). Injection molding was carried out on a TRX 80 Eco machine (Tederic, China) under the following conditions for all compositions: zone temperatures of 180, 185, and 200 °C, with a nozzle temperature of 200 °C. Additional processing parameters included a mold temperature of 35 °C, injection pressure of 36 bar, and a cooling time of 20 s.

Infrared spectroscopy was performed using a Nicolet iS10 FTIR spectrophotometer (Thermo Scientific, USA) in attenuated total reflection mode (ATR-FTIR). Each spectrum represents the average of 16 scans collected over the wavenumber range 4000–500 cm⁻¹.

Material densities were measured using a MVP-D160E gas pycnometer (Quantachrome Instruments, USA) with helium as the probe gas.

The reported values correspond to the mean of three independent measurements.

Mechanical characterization included tensile and flexural testing on an Instron 3367 machine (Instron, USA) at strain rates of 50 mm/min and 10 mm/min, respectively. Tensile tests were conducted on standardized paddle-shaped specimens, whereas flexural tests used bars (80 × 10 × 4 mm) supported at both ends (three-point bending mode). Twelve replicates were analyzed per material, and the mean values are reported.

Fracture surfaces were examined via optical microscopy VHX7000 (KEYENCE, Belgium) and scanning electron microscopy Phenom XL (Thermo Scientific, USA). SEM imaging was performed at 300× magnification, 5 kV accelerating voltage, in mapping mode using a backscatter electron detector (BSD Full) under high vacuum (0.1 Pa). The specimens were sputter-coated with gold for 60 s using a SEC MCM100P coater (SEC, South Korea). Final fracture surface images were generated by stitching 24 individual SEM micrographs using the microscope software.

Charpy impact testing was performed using an XJ 5Z impact tester (Liangong, China) equipped with a 2 J hammer, operating at a falling speed of 2.9 m/s. The tests were conducted on bar-shaped specimens (80 × 10 × 4 mm) cut from the measuring section of the paddle-shaped samples produced via injection molding. The unnotched impact strength (a_u) was determined for each specimen. Twelve replicates were tested for
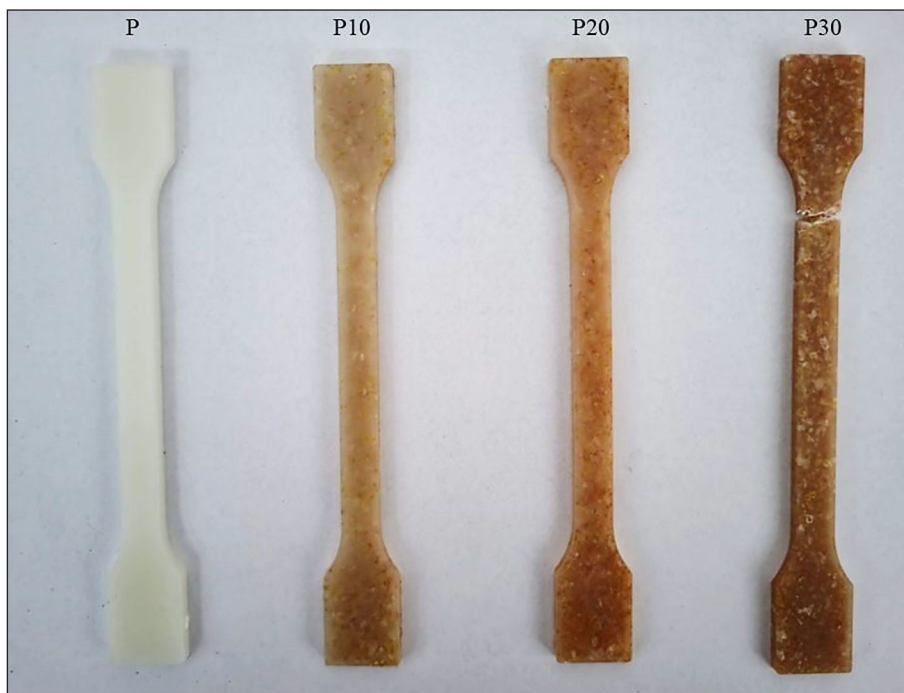
Figure 2. Test samples made by injection molding

each material, and the reported values correspond to the arithmetic mean of the measurements.

Thermomechanical analysis (DMA) was performed using a Q800 dynamic mechanical analyzer (TA Instruments, USA). Measurements were conducted over a temperature range of 30–150 °C with a heating rate of 3 °C/min. Bar-shaped specimens (60 × 10 × 4 mm), cut from the measuring section of the paddle-shaped samples obtained via injection molding, were used. The applied strain was 15 µm, and the oscillation frequency was 1 Hz.

Differential scanning calorimetry (DSC) analyses were carried out using a Q200 calorimeter (TA Instruments, USA) under a nitrogen atmosphere, over a temperature range of –60 to 220 °C with a heating/cooling rate of 10 °C/min. The samples with mass between 9.3 and 9.6 mg were subjected to three thermal cycles: first heating, cooling, and second heating. The first heating step aimed to eliminate the thermal history of the materialsinduced during the processing stage. From the cooling and second heating curves, the glass transition temperature (T_g), crystallization temperature (T_c), crystallization enthalpy change (ΔH_c), melting temperature (T_m), melting enthalpy change (ΔH_m), and degree of crystallinity (X_c) were determined using the TA Universal Analysis software. The degree of crystallinity (X_c) was calculated according to Equation 1.

$$X_c = \left(\frac{\Delta H_m}{\Delta H_{m100\%} \cdot (1-x)} \right) \cdot 100\% \qquad (1)$$

where: $\Delta H_{m100\%}$ – value of the enthalpy change of 100% crystalline PP; 207 J/g [18],
x – filler content.

Thermogravimetric analysis (TGA) was conducted using a Q500 thermobalance (TA Instruments, USA) under a nitrogen atmosphere over a temperature range of 25–700 °C, with a heating rate of 10 °C/min. Sample masses ranged from 21.2 to 22.2 mg. From the thermogravimetric curves, the temperatures corresponding to 5%, 50%, and 95% mass loss ($T_{5\%}$, $T_{50\%}$, and $T_{95\%}$, respectively) were determined. The $T_{5\%}$ value was used as an indicator of the thermal stability of the material (T_d). Additionally, the temperatures of maximum mass loss rates (T_{max}) for individual degradation stages were derived from the differential thermogravimetric (DTG) curve, obtained as the first derivative of the TG curve.

RESULTS AND DISCUSSION

FTIR analysis

Due to the lack of detailed information about the type of polymers constituting the photopolymer

printing matrices used in the research, an FTIR analysis was first performed to approximate the composition of the matrices. Since the input material constituting a potential filler for polymeric materials consisted of many printing matrices from different manufacturers and from different operational periods, several FTIR spectra measurements were made. The matrices turned out to be materially homogeneous, as most of the obtained spectra were very similar to each other. The main differences (if any) were limited primarily to slight differences in the absorbance of individual bands. Therefore, Figure 3 shows the average FTIR spectra of the stamp and reverse sides of the photopolymer printing matrices, and the presented analysis will refer to all the matrices tested.

According to the multi-material and layered structure of photopolymer printing matrices described in the introduction section, the FTIR spectra of the stamp side (Figure 3a) and the reverse side (Figure 3b) were different. The spectrophotometer software assigned the obtained spectra to: styrene-butadiene block copolymer (stamp side) and terephthalic acid-based polyester (reverse side). The identified polymers are typically used in the production of photopolymer printing matrices, therefore it can be assumed that the identification is correct. The styrene-butadiene copolymer constitutes the curable layer, while the polyesters act as the protective/ support layer.

To validate the software-based identification, an independent analysis of the acquired spectra was performed. This analysis confirmed the correct identification of the styrene-butadiene copolymer, as the observed spectra were consistent with literature data [19–21]. The broad absorption band at 3410 cm^{-1} corresponds to –O–H stretching vibrations of hydroxyl groups. The –CH stretching vibrations of both alkyl and aromatic moieties were observed at 2921 and 2850 cm^{-1}. A distinct peak at 1731 cm^{-1} is attributed to C=O stretching, indicating the presence of ester linkages in the polymer. Furthermore, the bands at 967, 909, and 757 cm^{-1} are characteristic of trans-1,4-, 1,2- and cis-1,4-polybutadiene, respectively, while the band at 699 cm^{-1} is typical of the benzene ring of polystyrene.

Also, the FTIR spectrum identified as polyester is in agreement with literature reports for this class of polymers [22–24]. The absorption bands at 2968 and 2905 cm^{-1} correspond to the symmetric and asymmetric stretching vibrations of C–H bonds. Prominent bands at 1717, 1262, 1125, and 1101 cm^{-1} are attributed to C=O and C–C–O stretching vibrations, reflecting the presence of ester groups within the copolymer. The band at 1410 cm^{-1} indicates aromatic ring vibrations, while bands at 1341 and 1021 cm^{-1} correspond to ester or carboxylic anhydride groups. The 1021 cm^{-1} band also reflects O=C–O–C
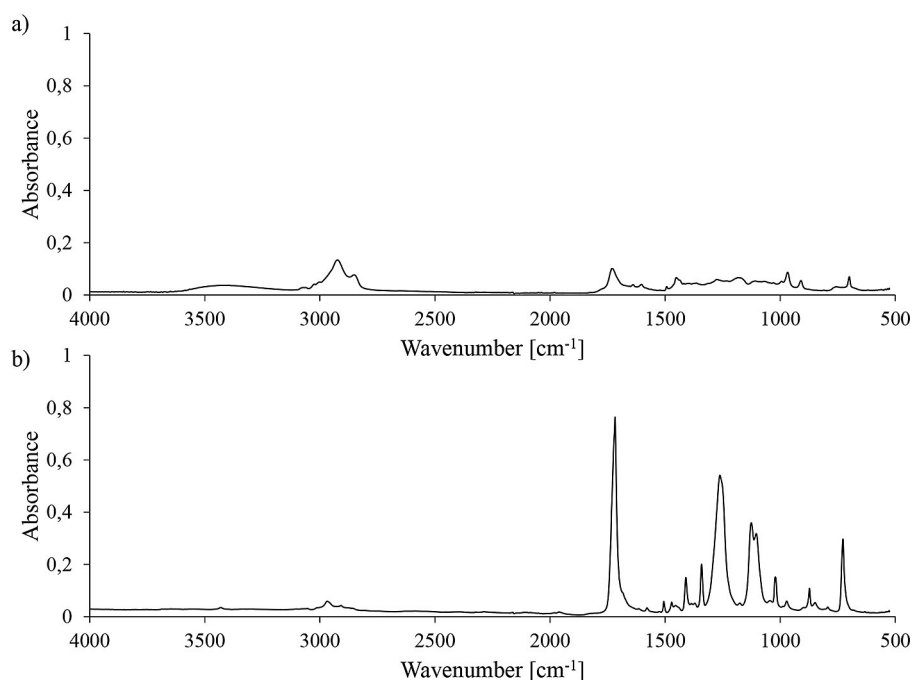

Figure 3. FTIR spectra of photopolymer printing matrices a) stamp side, b) reverse side

linkages, and the band at 971 cm^{-1} is assigned to C=C stretching. The absorption at 872 cm^{-1} is characteristic of five-substituted hydrogen atoms on the benzene ring, and the band at 728 cm^{-1} corresponds to C–H bending vibrations.

In addition to the printing matrices themselves, the spectra of pure PP and te materials containing shredded printing matrices were also obtained and analyzed. Figure 4 shows the spectra of samples P and P30. For greater readability, the spectra of other materials were not presented, but they were similar.

The FTIR spectra of pure polypropylene (PP) and the composites containing shredded printing matrices were found to be essentially identical, irrespective of the filler content. The spectra predominantly exhibited the bands characteristic of PP, with only minor variations in peak intensities. The observed bands include 2951, 2919, and 2838 cm^{-1}, corresponding to –CH stretching vibrations; 1457 and 1377 cm^{-1}, attributed to CH$_2$ bending and symmetric CH$_3$ deformation specific to polypropylene; 1168 cm^{-1}, corresponding to C–C bending inherent to the PP backbone; and 998, 973, and 842 cm^{-1}, indicative of isotactic polypropylene [25,26].

The lack of new bands in the spectra of samples P10, P20 and P30 indicates the lack of chemical interaction between the matrix (PP) and the filler (shredded photopolymer printing matrices). It therefore appears that the filler particles are only physically bound to the matrix material, which may be less advantageous when it comes to the potential mechanical properties of new materials.

Density

The feature that distinguishes pure polypropylene from most other polymers is its low density, usually from 0.895 to 0.920 g/cm^3 (depending on the type, production and processing methods). The experimentally determined density of the PP type used in the presented studies was 0.896 g/cm^3, so it was within the range typical for this polymer. The shredded waste of printing matrices was also characterized by a relatively low density of 1.058 g/cm^3. Therefore, its addition into the polymer, even in the highest amount assumed in the research plan, should not significantly increase the density of the composites in relation to the pure polymer. This is confirmed by the theoretical calculations of composite density carried out in accordance with the rule of mixtures. The experimentally determined density values were slightly lower than calculated theoretically, which could have resulted from the errors in dosing the filler in the extrusion process or the influence of injection process parameters (Figure 5). The determined density values of the tested composites were: 0.893 g/cm^3 for P10 (theoretical value 0.912 g/cm^3), 0.914 g/cm^3 for P20 (theoretical value 0.927 g/cm^3) and 0.928 g/cm^3 for P30 (theoretical value 0.943 g/cm^3).

The density analysis of the PP composites filled with waste material reveals a trend consistent with the principle of additive mixture, yet the observed experimental values were systematically lower than theoretical predictions. This deviation, attributable to the formation of interfacial voids resulting from poor matrix-filler adhesion,
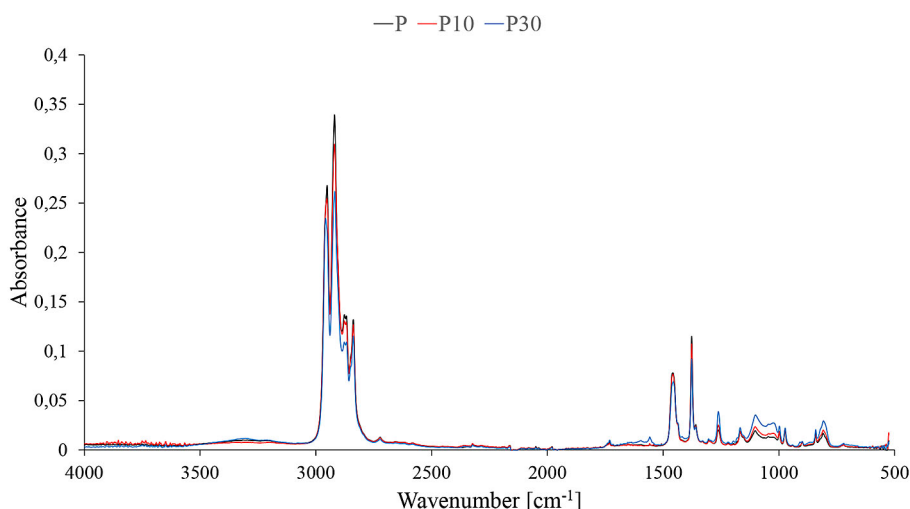

Figure 4. FTIR spectra of selected samples containing shredded photopolymer printing matrices
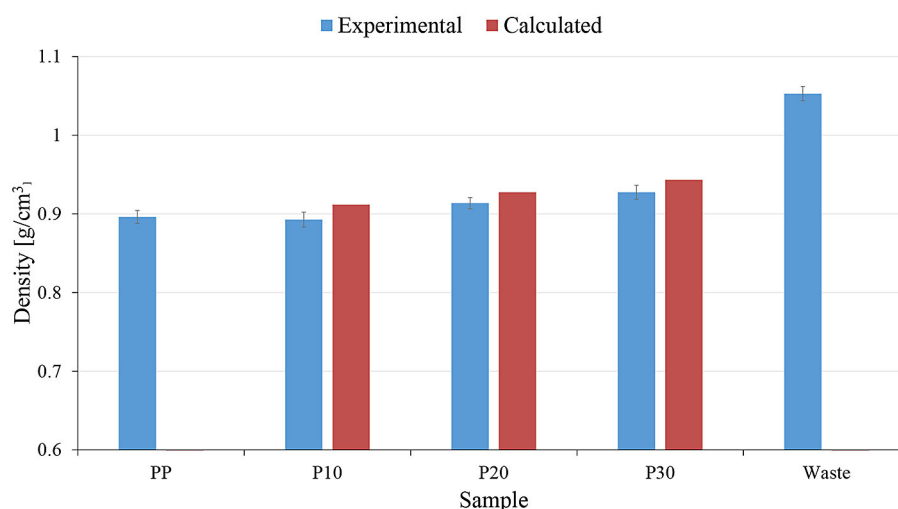
Figure 5. Density of the tested materials

aligns with the findings reporting on the epoxy composites incorporating a similarly prepared filler [15]. In contrast, the minimal density increase and maintenance of low specific weight even at high filler loadings are comparable to the results presented in [12], who noted only a marginal density change in PP composites with up to 15 wt.% filler. However, the more pronounced divergence from theoretical density in the present study, compared to the work [13] on polycaprolactone-based composites, underscores the critical influence of the specific polymer matrix and the absence of filler compatibilization. This comparison highlights that while the density behavior of such composites is generally predictable, the magnitude of structural imperfections – and thus the final material density – is highly dependent on the processing methodology and the intrinsic compatibility of the constituent phases. However, despite the high degree of filling of the composites, they are still characterized by low density, which makes it possible to produce low-weight shapes and products.

Mechanical properties

The mechanical properties of PP classify this polymer between polyethylene (PE) and engineering polymers. Compared to PE, polypropylene is stiffer and more resistant to stretching and bending. However, its impact strength is lower. The presented research focused on determining the impact of shredded photopolymer printing matrices on selected mechanical properties of the thus obtained composites.

Figure 6 shows the measurement results of selected stress and strain parameters.

The tensile strength (σ_M) of the pure PP samples was 22.7 MPa. Due to the physical state of PP at the test temperature (highly elastic state) and the occurrence of the necking phenomenon, the stress at break (σ_B) was significantly lower - 17.2 MPa. The photopolymer printing matrices were characterized by much better mechanical properties. The values of σ_M and σ_B determined in accordance with the direction of matrix production were 49.2 and 41.9 MPa, respectively. Therefore, it would seem that after addition into the polymer matrix, the mechanical parameters of the composites should be better than those of the pure polymer. Unfortunately, after grinding the waste printing matrices and adding it into the polymer matrix, a decrease in the mechanical parameters of the composites was observed.

The decrease in the mechanical parameters of the composites determined in the tensile test progressed with the increase in the content of shredded filler. The 10 wt.% of the filler (sample P10) reduced the tensile strength and stress at break to the level of 16.4 MPa, 20 wt.% of the filler (sample P20) to the level of 13.6 MPa, and 30 wt.% of the filler to the level of 10.9 MPa. The total decrease in tensile strength after the addition of the maximum filler content was therefore approximately 10 MPa, which is 50% of the initial value of pure PP.

Pure PP was characterized by a large difference between the strain at maximum stress (ε_M) and the strain at break (ε_B), which is typical for this polymer [27, 28]. The ε_M and ε_B values of sample
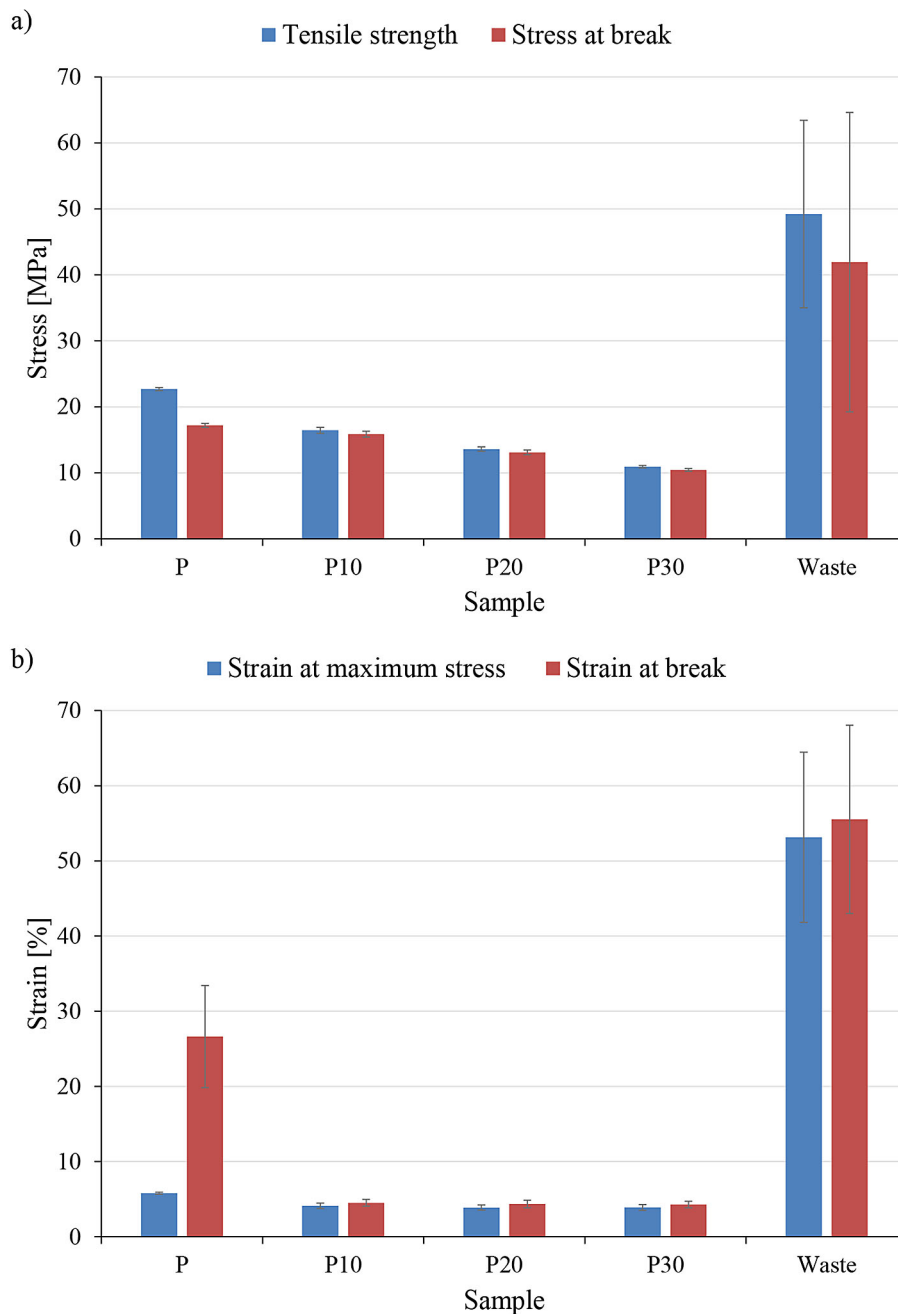
Figure 6. Results of measurement of a) stress, b) strain of the tested materials

P were 5.8 and 26.6%, respectively. Photopolymer printing matrices were characterized by high deformation values, where the recorded ε_M and ε_B were 53.1 and 55.5%, respectively. However, the addition of printing matrices in shredded form reduced the recorded strains, especially in the ε_B range.

The ε_M value decreased from 5.8% for sample P to 3.9% for sample P30, representing a 33% decrease in the value of pure PP. A much greater change was recorded for ε_B. Introduction of already 10 wt.% shredded filler reduced this parameter from 26.6% (sample P) to 4.5% (sample

P10). This is a decrease of as much as 83% compared to pure PP. Increasing the amount of filler in the composite did not cause any further significant changes in this parameter.

The recorded changes in mechanical parameters (stress and strain) obtained during the static tensile test are typical changes accompanying the addition of this partial filler to the polymer matrix, without prior modification of the filler or the use of special compatibilizers improving interfacial adhesion. Due to the presence of particles in the volume, stresses aggregate at the points of

matrix/filler contact. The lack of special preparation of the filler material means that the individual phases of the composite are poorly bonded to each other, which results in large amounts of empty spaces at the matrix/filler interface, which reduces the mechanical strength of the material. The presence of voids has been confirmed by SEM tests (Figure 7).

The minimal differences in strain observed among the composites containing fillers can be attributed to the presence of at least one filler particle within the cross-section of each specimen. Stress concentrations around these particles lead to sample failure prior to the onset of necking.

Consequently, the incorporation of shredded printing matrices into the polymer matrix also affected the elasticity of the materials. The addition of these fillers significantly reduced the Young's modulus of the resulting composites compared to that of pure PP (Figure 8).

Pure PP had a Young's modulus of 1290 MPa, while the printing matrices had a modulus of 1407 MPa. The recorded values of the Young's modulus of the obtained composites were 1060 MPa for sample P10, 975 MPa for sample P20 and 825 MPa for sample P30. It is therefore visible that the elasticity of the material decreased with the increase in the content of the filler used, and the total decrease at the maximum amount of filler was 33% in relation to the value of pure PP. This decline is attributed to poor interfacial adhesion between the non-polar PP matrix and the polar filler, leading to the formation of stress concentration points and voids, as confirmed by SEM analysis.

The reduction observed in this study is consistent with the patterns previously reported for the polymer composites containing elastomeric or poorly compatible waste-derived additives. For example, comparable declines in stiffness have been described for the polypropylene composites incorporating waste tire rubber, where the soft rubber inclusions function as compliant regions within the otherwise rigid matrix [29]. In contrast, the addition of rigid mineral waste fillers, such as fly ash or glass powder, generally enhances the Young's modulus of polyolefins [30]. This clear disparity highlights that the mechanical performance of waste-filled composites is not determined merely by filler loading, but is largely dependent on the intrinsic characteristics of the filler – most notably its stiffness – as well as the interfacial adhesion with the polymer matrix. Therefore, the findings presented here reflect
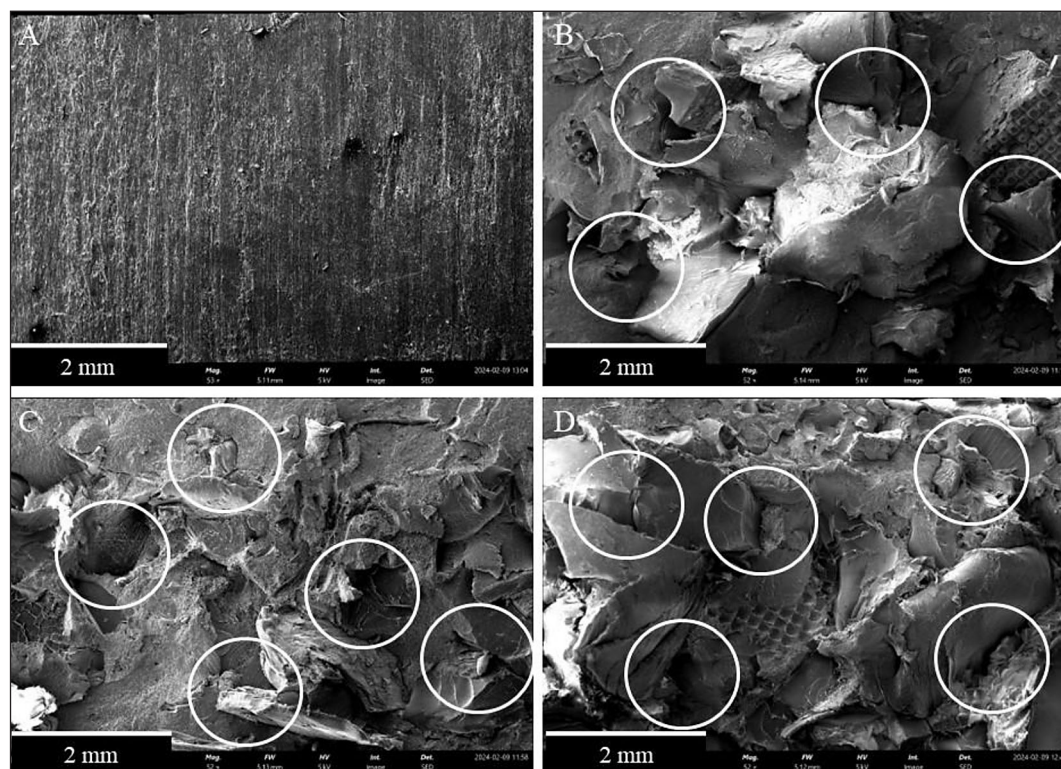

Figure 7. SEM images of the fracture of samples A – P; B–P10; C–P20; D–P30. Voids between the matrix and the filler are marked with white circles
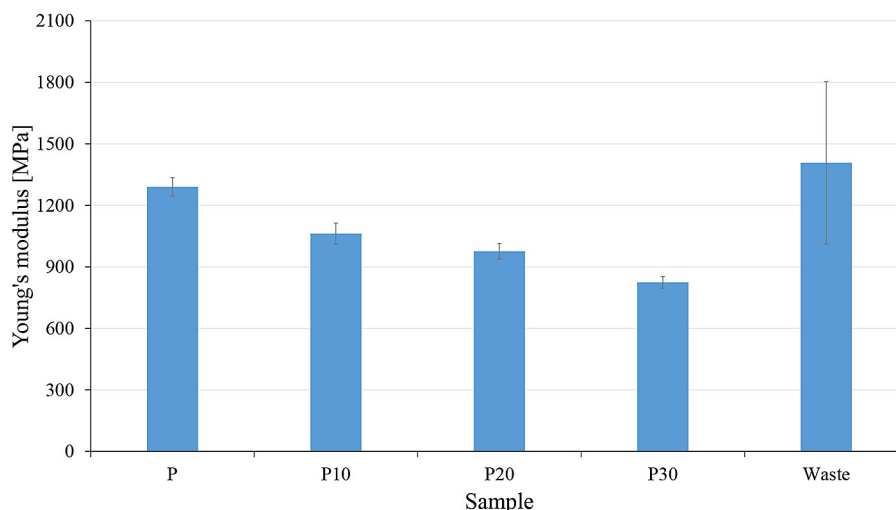
Figure 8. Young's modulus of the tested materials

a system in which a rigid matrix is combined with a softer and incompatible filler, resulting in a reduction of elastic properties.

The use of shredded printing matrices as a filler in polymeric materials also influenced the flexure strength of the produced composites (Figure 9).

The flexural strength (σ_F) of pure PP was 37 MPa with a strain at maximum flexural stress (ε_F) of 6.6%. Due to the specificity of photopolymer printing matrices, it was not possible to determine their bending properties. The tested photopolymer matrices were too flexible and did not have sufficient stiffness to be properly mounted in the bending holder of the testing machine. Hence, it was impossible to determine the parameters of these materials during the bending test.

The addition of shredded printing matrix particles into the polymer matrix resulted in an approximately linear decrease in flexural strength. Adding 10 wt.% of the filler (sample P10) reduced σ_F to 31 MPa, 20 wt.% of the filler (sample P20) to 27 MPa and 30 wt.% of the filler to 23 MPa. The total decrease in this parameter in the case of the highest filler content was 38% compared to the value of pure PP.

However, no significant effect was observed in the case of ε_F. Although a certain decrease was observed after the introduction of 20 wt.% of the filler, the recorded change was so small that it could be considered insignificant. It can therefore be concluded that the introduction of shredded printing matrix particles into the PP matrix did not affect the deformation at the maximum bending stress of the composites.

The observed reduction in tensile strength (50%) and flexural strength (38%) for the 30 wt.% composite aligns with the typical behavior of the polyolefin composites incorporating non-compatibilized, elastomeric waste materials. A similar decline in mechanical performance has been documented in other systems, such as the PP filled with recycled tire rubber and certain plastic blends or the PP composites with the addition of wood industry waste, where the lack of strong interfacial adhesion and the presence of soft, incompatible phases lead to inefficient stress transfer and premature failure [29]. On the other hand, there are examples in the literature where the use of waste leads to the reinforcement of the composite. For example, the addition of short recycled glass fibers to a polyamide matrix can significantly improve its mechanical properties, including tensile and flexural strength, owing to strong interactions at the fiber-polymer interface [31]. Similarly, the composites containing rigid mineral waste fillers (e.g., fly ash or glass powder) often exhibit an increase in stiffness and flexural strength, albeit frequently at the expense of impact toughness [32,33]. The results obtained in this study therefore situate the photopolymer waste within the category of the fillers that deteriorate the mechanical strength of a virgin PP matrix without compatibilization. This limitation could be addressed via surface modification or the use of coupling agents to transform this waste stream into a performant reinforcing agent.

The last mechanical parameter that is important for the possible applications of the obtained
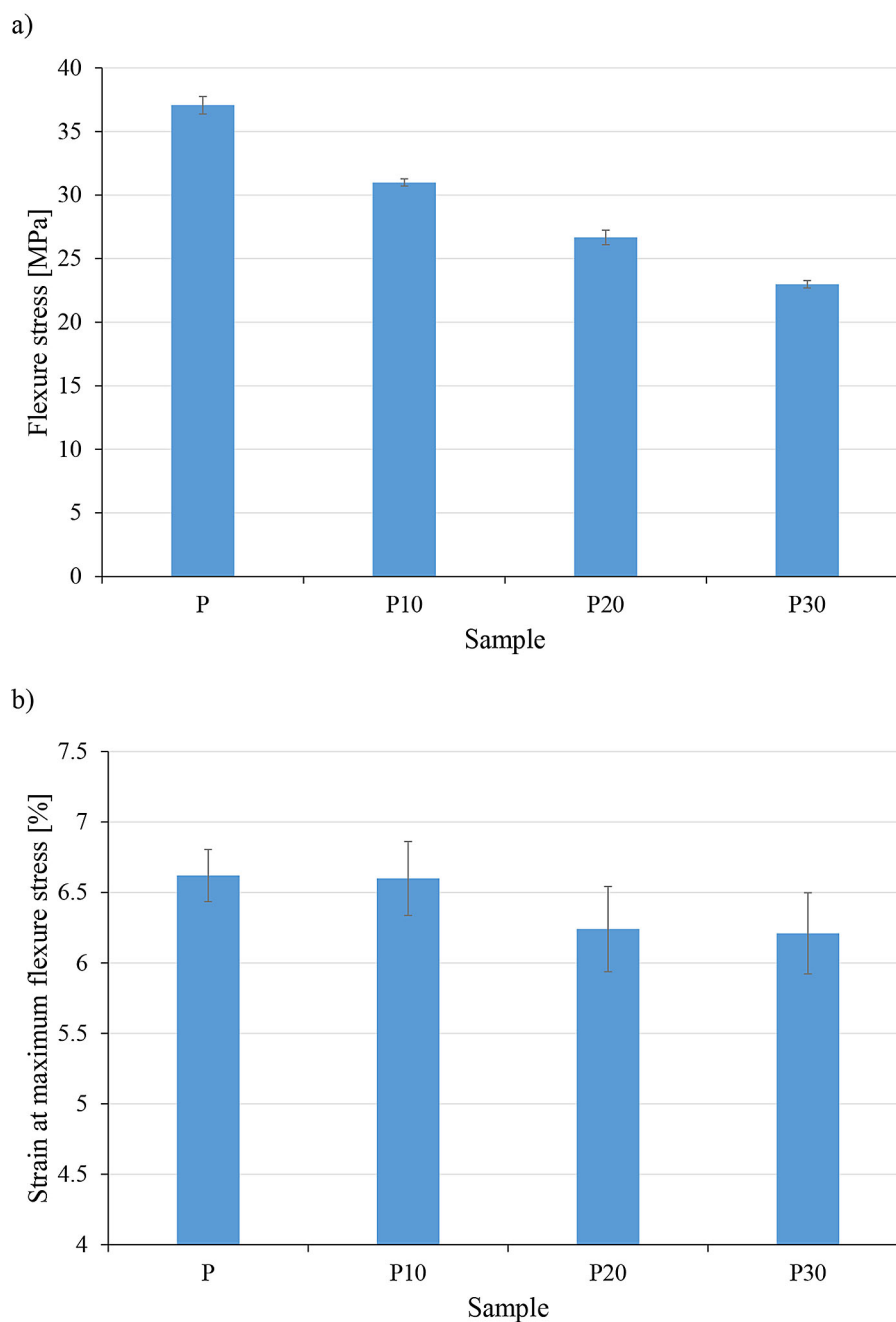
a)

b)

Figure 9. Measurement results of a) flexural stress,
b) strain at the maximum flexural stress of the tested materials

composites is impact strength (u_a). Pure PP (without notch) was not damaged during the Charpy's impact test. This is due to the high flexibility of this polymer, and therefore also high resistance to impact impacts. The u_a values of sample P recorded and shown in Figure 10 therefore correspond to the value of incomplete fracture (bending) of this material. As in the case of the bending test, the specificity of photopolymer printing matrices made it impossible to conduct an impact test for this material.

Even the lowest content of waste filler induced sample cracking upon impact. The measured unnotched impact strength (a_u) of the P10 sample was 35 kJ/m². Increasing the filler content led to a further reduction in impact strength: at 20 wt.% filler, a_u decreased to 21 kJ/m², and at 30 wt.% filler, it reached only 17 kJ/m². This corresponds to a maximum reduction of 67% relative to pure polypropylene.

The observed decrease in impact strength is attributed to the increased presence of filler
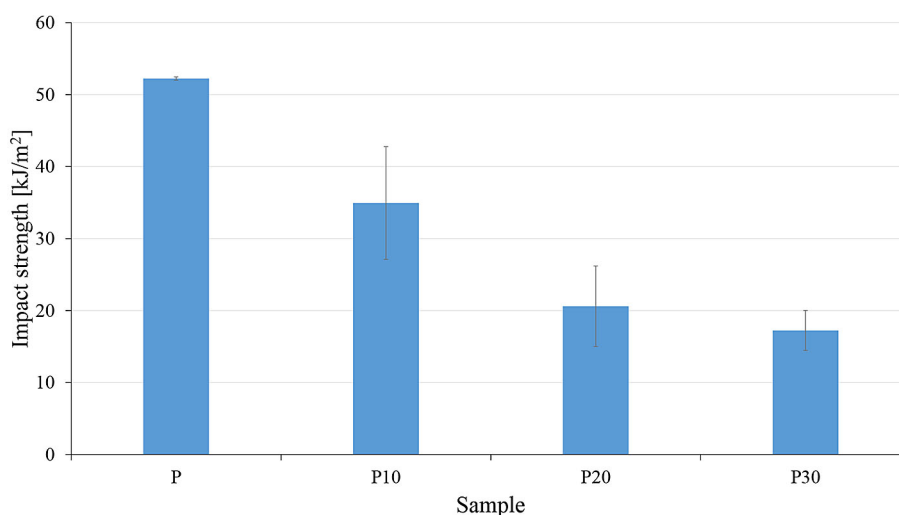
Figure 10. Impact strength of the tested materials

particles within the polymer matrix and consequently the sample cross-section, which reduces the effective polymer content and diminishes the overall toughness of the composite (Figure 11).

The analysis of the impact strength reveals a profound embrittlement of the polypropylene composites upon the incorporation of the shredded printing matrices. The decline in impact strength is significantly more pronounced than the reductions observed for tensile or flexural properties. The primary mechanism, as confirmed by SEM and optical microscopy, is the poor interfacial adhesion and the resulting void formation at the matrix-filler interface, which act as stress concentrators and initiate catastrophic crack propagation under high-strain-rate impact conditions. This phenomenon is well-documented in the literature for non-compatibilized polymer composites with weak interfacial bonding. Previous studies demonstrated that in the PP composites filled with rigid particles, the impact strength is critically dependent on the interface quality, where poor adhesion leads to decohesion and rapid failure [34]. Also in rubber-toughened systems, the efficiency of stress transfer and energy dissipation is paramount for impact resistance; in its absence, filler particles act as defects that severely compromise toughness [35, 36]. The results obtained in this study are, therefore, consistent with the established understanding that without effective interfacial modification, the incorporation of rigid or semi-rigid fillers, especially at high loadings, is detrimental to the impact performance of thermoplastic composites.

Thermomechanical properties

The mechanical performance of polymers and polymer composites is strongly temperature-dependent. Accordingly, the thermomechanical properties of the prepared composites were evaluated (Figure 12).

The storage modulus of pure PP determined at 30 °C (E'30) was 1000 MPa and decreased with increasing temperature, reaching the value of 217 MPa at 120 °C. At the same time, the damping coefficient (Tan Delta) increased with temperature, reaching a maximum around 110 °C. The recorded changes in the course of the curves are typical for thermoplastic polymer materials, in which the storage modulus decreases with increasing temperature, which is related to changes in the physical state of the polymers.

The printing matrices were characterized by lower variability of the storage modulus as a function of temperature, as this parameter decreased from 80 MPa at 30 °C to 60 MPa at 120 °C. The damping coefficient increased significantly after exceeding 60 °C.

The addition of shredded filler particles reduced the storage modulus of the obtained composites over the entire temperature range, while not significantly affecting the characteristics of the thermomechanical and damping coefficient curves. The observed changes in the storage modulus after the introduction of the filler are partially in line with expectations. Comparing the modulus values of pure PP (high modulus) and the polymer printing matrix (low modulus), it could be expected that the composites created
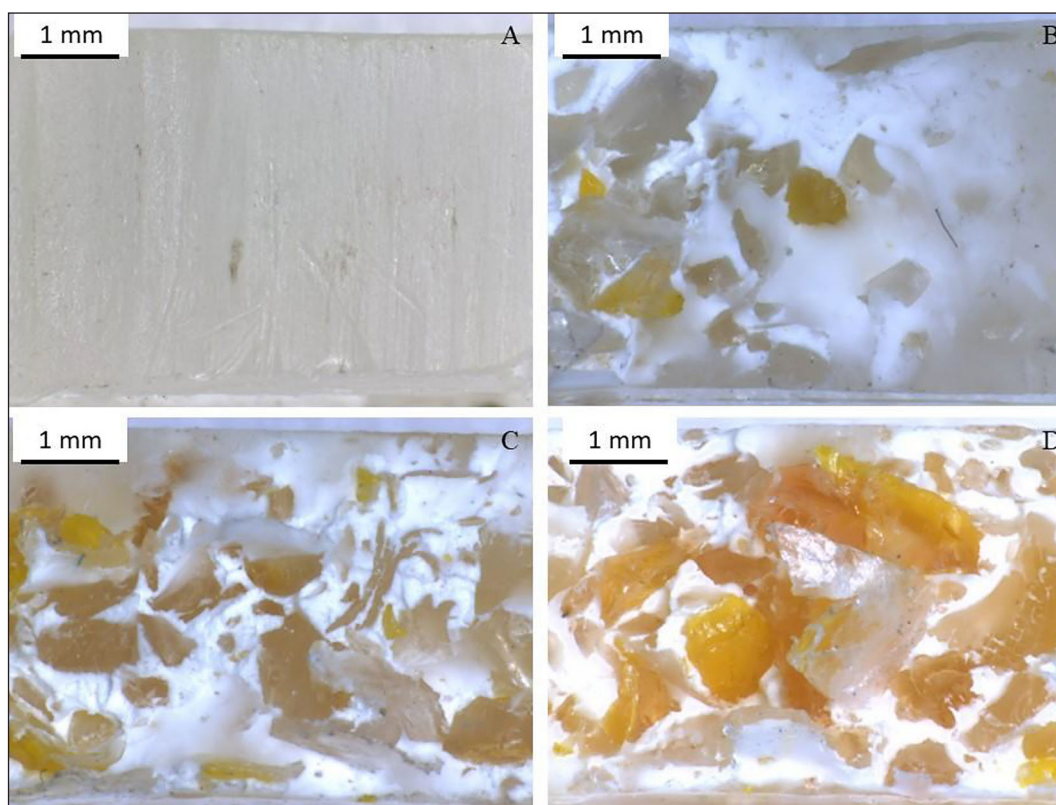
Figure 11. Microscopic photos of cross-sections of samples A - P, B - P10, C - P20, D - P30

would be characterized by intermediate values, with the higher the filler content, the lower the storage modulus value. Therefore, as described above, the recorded storage modulus at 30 °C decreased to 921 MPa after adding 10 wt.% of filler, 840 MPa after adding 20 wt.% of filler and 781 MPa after adding 30 wt.% of filler. The maximum modulus decrease was therefore 22%, compared to pure PP, and remained at a similar level throughout the entire test temperature range.

Furthermore, the shape and position of the tan δ peak remained largely unchanged. This indicates that the segmental mobility of the polymer chains was not restricted by the filler, a phenomenon observed when there is no strong interfacial interaction or when the filler does not influence the polymer relaxation dynamics. This finding aligns with the work on waste-filled composites, which reported that the fillers which do not chemically interact with the matrix primarily affect the
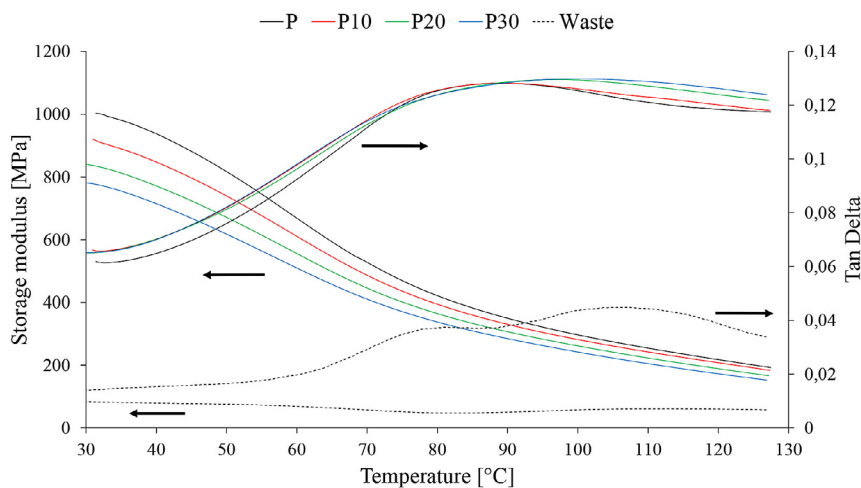

Figure 12. Thermomechanical curves of the tested materials

mechanical performance through their physical presence and the resulting stress concentrations, without altering the fundamental viscoelastic transitions of the polymer [37]. Consequently, the DMA results conclusively show that the unmodified waste filler plasticizes the composite structure from a dynamic mechanical perspective, reducing its stiffness without enhancing the damping characteristics or restricting molecular motion within the PP matrix.

Thermal properties

In addition to the mechanical properties of polymer materials, their thermal properties are also of great importance. It is important, among other things, to understand the temperatures, the nature and intensity of phase changes occurring during temperature changes, as well as the thermal resistance of the obtained materials. Table 1 summarizes the results of differential scanning calorimetry (DSC) and thermogravimetric analysis (TGA) of the tested samples and the photopolymer printing matrix.

Figure 13 shows the thermal curves of cooling and second heating of the tested polymer materials. The first heating was intended to remove the thermal history of the samples and is therefore not shown.

In the obtained thermal curves of pure PP (sample P), only the peaks related to the crystallization process (cooling curve, exothermic reaction) and the melting process of the crystalline phase (heating curve, endothermic reaction) were recorded. The determined crystallization temperatures (T_c) and melting temperatures (T_m) were 123.9 and 164.2°C, respectively, and the degree of crystallinity of sample P determined from formula (1) was 44.7%. Despite the use of the lower test range up to -60 °C, it was not possible to register a change in the curve related to the glass transition of PP, which, according to the literature, occurs at approximately -20 °C [28]. In the case of the printing matrix, no peaks or changes indicating the occurrence of thermal phenomena were recorded in the thermal curves. Therefore, it can be concluded that no phase transformations occur in this material in the temperature range used.

As for the influence of the filler on phase transformations, it manifests itself most during the cooling of the tested materials. The introduction of a shredded printing matrix lowered the crystallization temperature. The content of 10 wt.% of filler reduced the T_c to 119.7 °C, 20 wt.% filler to 118.0 °C and 30 wt.% filler to 117.3 °C. Therefore, the crystallization temperature decreased by as much as 6.6 °C when using the maximum filler content. The delay in the crystallization process was probably due to the fact that the filler particles contained in the matrix hindered the movement of the macromolecules of the polymer matrix, which resulted in the observed changes in the crystallization temperature. The thermal effects of the crystallization process were also smaller. A decrease in the value of enthalpy changes in the crystallization process (ΔH_c) was observed, but this was rather the effect of a smaller amount of the PP phase in the entire volume of the sample, with an increasing content of the thermally neutral filler.

However, the filler had a smaller impact on the melting process of the tested materials. Only a slight decrease in T_m was recorded. This value decreased by less than 2 °C only after introducing the highest content of shredded printing matrix. Again, the thermal effects accompanying the melting process were also smaller, but this was also due to the lower content of the polymer phase in the entire volume of the tested samples.

The filler also did not significantly affect the degree of crystallinity of the obtained materials compared to pure PP. There was no relationship between the content of the crystalline phase and the amount of filler, and the calculated X_c values of samples P10, P20 and P30 were similar to the value obtained for sample P.

Table 1. Selected thermal parameters of the tested materials

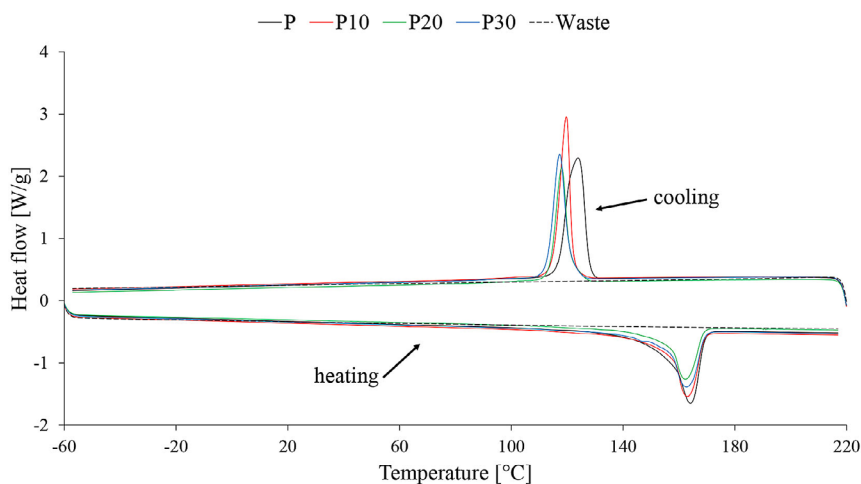| Sample	T_d [°C]	T_c [°C]	ΔH_c [J/g]	T_m [°C]	ΔH_c [J/g]	X_c [%]
P	363.4	123.9	94.6	164.2	92.5	44.7
P10	371.6	119.7	81.4	163.0	80.0	42.9
P20	378.9	118.0	64.5	162.2	63.2	38.2
P30	386.8	117.3	72.9	162.7	71.1	49.1
Waste	395.0	-	-	-	-	-

Figure 13. Thermal curves of the tested materials; exo up

The observed thermal behavior is consistent with the findings reported for other polypropylene composites filled with waste materials, such as ground tire rubber (GTR), where the filler particles similarly restricted the mobility of polymer chains, leading to a decrease in T_c [38]. However, it should be noted that the effect of waste fillers is not always unequivocal. In contrast to the present results, examples exist in the literature where wastes such as wood flour or fly ash act as nucleating agents, accelerating crystallization and consequently increasing its temperature [32,39]. The impact of the filler on the T_m and the X_c values was negligible, suggesting that the presence of ground printing matrices does not significantly disrupt the final crystalline structure of polypropylene. A similar lack of significant changes in X_c has been observed for the PP composites containing the aforementioned GTR. It can therefore be inferred that the investigated waste filler primarily acts as a steric hindrance to polymer chain mobility rather than as an active nucleating agent, a phenomenon that has been well documented for certain types of fillers in polymer matrices.

The tests also determined the thermal resistance and the degradation process of the tested materials. Figure 14 shows the thermogravimetric curves of the tested samples and the shredded polymer printing matrix.

The thermal resistance of pure PP, defined as the temperature at which 5% of the sample mass was lost ($T_{5\%}$), was 363.4 °C. The degradation process of the P sample occurred in one stage in the range from 280 to 510 °C, with the maximum intensity at 453.7 °C. During the thermal degradation process, the tested material completely disintegrated, as no residue was recorded. The polymer matrices were characterized by a higher thermal resistance than pure PP, because the recorded $T_{5\%}$ value of the filler was 395.0 °C, and therefore was almost 32 °C higher than that recorded for the P sample. However, the degradation process itself was the same as in the case of PP. The degradation occurred in one stage in the temperature range from 320 to 500 °C, with maximum intensity at 468.0 °C. Also in the case of printing matrices, no residue remained after the degradation process.

As it could be expected, the introduction of filler particles, which were characterized by higher thermal resistance, resulted in an increase in the $T_{5\%}$ value of the obtained materials compared to pure PP. The addition of 10 wt.% of the filler resulted in an increase in $T_{5\%}$ to 371.6 °C, the addition of 20 wt.% of the filler increased it to 378.9 °C and the addition of 30 wt.% of the filler increased it to 386.8 °C. The maximum increase in thermal resistance was therefore 23.4 °C when using the largest amount of filler. The observed increase in thermal resistance was therefore a direct consequence of the increasing amount of a more thermally resistant phase in the entire volume of the obtained materials. This improvement is consistent with reports for other systems where a filler possesses higher thermal stability than the matrix, leading to a synergistic or at least an additive effect. A similarly beneficial trend was observed for the polyethylene composites filled with ground electronic waste (PCB) or modified shell waste, where the filler acted as a thermal barrier [40,41]. Conversely,
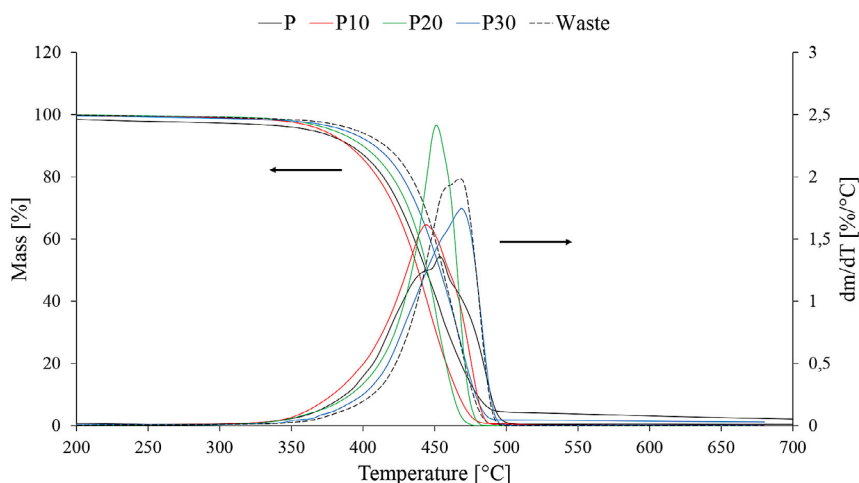
Figure 14. Thermogravimetric curves of the tested materials

in the polypropylene composites modified with residual tire rubber crumbs, an increase in thermal stability has also been reported, which was attributed to the rubber particles acting as a carbon source that forms a protective layer during heating [29].

Although the already recorded thermal resistance of pure PP is sufficient for all typical applications of this polymer, the greater thermal resistance of the obtained materials is not without significance. Firstly, the increase in thermal resistance increases the resistance of a material to increased temperatures, which allows the scope of possible applications of new materials to be expanded. Secondly, higher thermal resistance facilitates processing, owing to the need to maintain a lower temperature regime, the phenomenon of overheating of the polymer melt is reduced, which consequently leads to better quality products. The TGA results confirm that polymer waste, even without surface modification, can effectively improve the thermal resistance of materials, thereby broadening their application potential within a circular economy framework.

Even considering the observed reduction in mechanical properties, the obtained composites could find application in a range of areas where top-tier mechanical strength is not the primary requirement, but low density and enhanced thermal stability are advantageous. The proposed material could potentially be suitable for use as a core material for lightweight, non-load-bearing construction panels, employed in furniture or interior partitions. The high waste filler content and the associated reduced weight could be a significant advantage in such scenarios.

Furthermore, the composites could be appropriate for the production of rigid packaging that is not subject to significant mechanical loads, while their increased thermal resistance would facilitate injection molding processes and ensure shape stability. The introduction of such a substantial amount of waste into the material cycle in the form of a new product would represent a realization of circular economy principles, allowing for a reduction in virgin polymer consumption in applications with lower performance requirements.

Subsequent research would focus on improving the interfacial adhesion, which could potentially broaden the scope of applications to components subjected to higher loads. Future research should prioritize the use of compatibilizers to mitigate the poor interfacial adhesion identified in this study. The most straightforward candidate is maleic anhydride-grafted polypropylene (MAPP), a well-established standard for enhancing the compatibility between PP and polar fillers by acting as a molecular bridge [29]. Beyond MAPP, exploring other graft copolymers could yield further improvements. For instance, styrene-ethylene/butylene-styrene grafted with maleic anhydride (SEBS-g-MA) could simultaneously improve toughness and adhesion, while polypropylene grafted with acrylic acid (PP-g-AA) may offer alternative interactions with the filler surface chemistry [32, 42]. The systematic application of these agents is a critical next step to transform the waste filler from a passive diluent into an active reinforcement, unlocking the full potential of these sustainable composites.

CONCLUSIONS

The primary objective of the study was successfully achieved. Waste photopolymer printing matrices, a significant post-production waste from the printing industry, can be effectively utilized as a filler in polypropylene composites, supporting circular economy principles. The addition of shredded waste material of photopolymer printing matrices to a polypropylene matrix influenced the selected physical, mechanical, and thermal properties of the resulting composites:

The density of the composites increased with the filler content; however, even at high levels of reinforcement, all materials remained of relatively low density (<1 g/cm³).

The decline in mechanical properties progressed with increasing filler content. At the highest filler loading, reductions of 50%, 33%, 38%, and 67% were observed for tensile strength, Young's modulus, flexural strength, and impact strength, respectively, relative to pure polypropylene. The diminished mechanical performance is likely attributable to the absence of specialized filler treatment, resulting in poor interfacial adhesion between the matrix and filler as well as the formation of voids at the matrix/filler interface.

Storage modulus of the composites decreased over the entire temperature range with the addition of the filler, with a maximum reduction of 22% compared to pure PP. The general shape of the thermomechanical curves was not significantly altered.

The filler particles hindered the mobility of the polymer chains, resulting in a lower crystallization temperature (a decrease of up to 6.6 °C). This retardation of crystallization is attributed to the presence of filler particles, which impede the mobility of polymer macromolecules and thereby hinder their arrangement. The filler itself showed no thermal transitions in the analyzed range.

The addition of the filler, which has a higher intrinsic thermal stability than PP, significantly improved the thermal resistance of the composites. The temperature of 5% mass loss ($T_{5\%}$) increased by up to 23.4 °C.

It is evident that the incorporation of printing waste leads to a deterioration of the material properties; however, the observed reductions remain acceptable for the intended applications of the developed composites. It should be emphasized that the primary objective of this study was to valorize the post-production waste generated during label manufacturing, which was successfully achieved through its use as a polymer filler. Enhanced properties of the composites containing printing waste could potentially be attained through prior modification of the filler, which will be addressed in future research.

REFERENCES

1. Camacho-Otero J, Boks C, Pettersen IN. Consumption in the Circular Economy: A Literature Review. Sustain 2018;10:2758. https://doi.org/10.3390/SU10082758

2. Morseletto P. Targets for a circular economy. Resour Conserv Recycl 2020;153:104553. https://doi.org/10.1016/J.RESCONREC.2019.104553.

3. Webster K. A Circular Economy Is About the Economy. Circ Econ Sustain 2021;1:115–26. https://doi.org/10.1007/S43615-021-00034-Z/FIGURES/3

4. Stahel WR, MacArthur Foundation E, Ellen MacArthur D. The Circular Economy : A User's Guide. New York : Routledge, 2019: Routledge; 2019. https://doi.org/10.4324/9780429259203

5. EUR-Lex - 52020DC0098 - EN - EUR-Lex n.d. https://eur-lex.europa.eu/legal-content/EN/TXT/?qid=1583933814386&uri=COM:2020:98:FIN (accessed March 19, 2024).

6. Hayta P, Oktav M. The Importance of Waste and Environment Management in Printing Industry. Eur J Eng Nat Sci 2019;3:18–26.

7. Alabdulhadi A, Ramadan A, Devey P, Boggess M, Guest M. Inhalation exposure to volatile organic compounds in the printing industry. J Air Waste Manage Assoc 2019;69:1142–69. https://doi.org/10.1080/10962247.2019.1629355.

8. Hansuebsai A, Kaosod A, Kanchanasing T. A new environmental performance index based on the carbon footprint, VOC emissions, and waste in a printing house. Eng Reports 2020;2:e12165. https://doi.org/10.1002/ENG2.12165

9. Carlos Alberto PJ, Sonia Karina PJ, Francisca Irene SA, Adrielly Nahomee RÁ. Waste reduction in printing process by implementing a video inspection system as a human machine interface. Procedia Comput Sci 2021;180:79–85. https://doi.org/10.1016/J.PROCS.2021.01.131

10. Charoensopa K, Wajima T, Hansuebsai A. Waste Management in Printing Houses by producing Activated Carbon from wastepaper to treat wastewaters. J Print Sci Technol 2023;60:360–4. https://doi.org/10.11413/NIG.60.360

11. Liu X, Guthrie JT. A review of flexographic printing plate development. Surf Coatings Int Part B Coatings Trans 2003;86:91–9. https://doi.org/10.1007/BF02699619/METRICS

12. Cordeiro CC, Bernardin AM, Da Silva L, Fiori MA, Benavides R, Oenning LW, et al. A study of the recycling and stability of flexographic photopolymer plates. J Appl Polym Sci 2010;118:1436–41. https://doi.org/10.1002/APP.32406

13. Gürler N, Pekdemir ME, Torğut G, Kök M. Binary PCL–waste photopolymer blends for biodegradable food packaging applications. J Mol Struct 2023;1279:134990. https://doi.org/10.1016/J.MOLSTRUC.2023.134990

14. Kök BV, İrhan B, Yılmaz M, Yalçın E. Research on the rheological properties of bitumen modified with waste photopolymer. Constr Build Mater 2022;346:128446. https://doi.org/10.1016/J.CONBUILDMAT.2022.128446

15. Ferretto A, Zimmermann MVG, Filho NLD, de Almeida MK, Angioletto E. Influence of the incorporation of flexographic photopolymer plate residues on the mechanical properties of epoxy. REM - Int Eng J 2023;76:169–76. https://doi.org/10.1590/0370-44672022760038

16. Zimmermann MVG, de Almeira MK, Ponsoni LV, Bernardo MA, Zattera AJ, Beltrami LVR, et al. Influence of flexographic photopolymer-plate residue incorporation on the mechanical properties of glass-fiber-reinforced polyester composites. Mater Res 2023;26:e20230239. https://doi.org/10.1590/1980-5373-MR-2023-0239

17. Moraczewski K, Karasiewicz T, Suwała A, Bolewski B, Szabliński K, Zaborowska M. Versatile Polypropylene Composite Containing Post-Printing Waste. Polym 2022;14:5335. https://doi.org/10.3390/POLYM14245335

18. Lanyi FJ, Wenzke N, Kaschta J, Schubert DW. On the determination of the enthalpy of fusion of α-crystalline isotactic polypropylene using differential scanning calorimetry, x-ray diffraction, and Fourier-transform infrared spectroscopy: An old story revisited. Adv Eng Mater 2020;22:1900796. https://doi.org/10.1002/ADEM.201900796

19. Wang F, Chang L, Hu Y, Wu G, Liu H. Synthesis and Properties of In-Situ Bulk High Impact Polystyrene Toughened by High cis-1,4 Polybutadiene. Polym 2019;11:791. https://doi.org/10.3390/POLYM11050791

20. Min X, Fan X. A new strategy for the synthesis of hydroxyl terminated polystyrene-b-Polybutadiene-b-Polystyrene triblock copolymer with high Cis-1, 4 content. Polym 2019;11:598. https://doi.org/10.3390/POLYM11040598

21. Khan A, Kian LK, Jawaid M, Khan AAP, Alotaibi MM, Asiri AM, et al. Preparation of styrene-butadiene rubber (SBR) composite incorporated with collagen-functionalized graphene oxide for green tire application. Gels 2022;8:161. https://doi.org/10.3390/GELS8030161/S1

22. Smith BC. Infrared Spectroscopy of Polymers, VIII: Polyesters and the Rule of Three. Spectrosc (Santa Monica) 2022;37:25–8. https://doi.org/10.56530/SPECTROSCOPY.TA9383E3

23. Parvinzadeh M, Ebrahimi I. Influence of atmospheric-air plasma on the coating of a nonionic lubricating agent on polyester fiber. Radiat Eff Defects Solids 2011;166:408–16. https://doi.org/10.1080/10420150.2011.553230

24. Kirshanov K, Toms R, Melnikov P, Gervald A. Unsaturated polyester resin nanocomposites based on post-consumer polyethylene terephthalate. Polymers (Basel) 2022;14:1602. https://doi.org/10.3390/POLYM14081602/S1

25. Gopanna A, Mandapati RN, Thomas SP, Rajan K, Chavali M. Fourier transform infrared spectroscopy (FTIR), Raman spectroscopy and wide-angle X-ray scattering (WAXS) of polypropylene (PP)/cyclic olefin copolymer (COC) blends for qualitative and quantitative analysis. Polym Bull 2019;76:4259–74. https://doi.org/10.1007/S00289-018-2599-0/FIGURES/10

26. Smith BC. The infrared spectra of polymers III: Hydrocarbon polymers. Spectrosc (Santa Monica) 2021;36:22–5. https://doi.org/10.56530/SPECTROSCOPY.MH7872Q7

27. Shubhra QTH, Alam AKMM, Quaiyyum MA. Mechanical properties of polypropylene composites. Http://DxDoiOrg/101177/0892705711428659 2011;26:362–91. https://doi.org/10.1177/0892705711428659

28. Maddah HA. Polypropylene as a Promising Plastic: A Review. Am J Polym Sci 2016;6:1–11. https://doi.org/10.5923/J.AJPS.20160601.01.

29. Chiang TC, Liu HL, Tsai LC, Jiang T, Ma N, Tsai FC. Improvement of the mechanical property and thermal stability of polypropylene/recycled rubber composite by chemical modification and physical blending. Sci Rep 2020;10:1–8. https://doi.org/10.1038/S41598-020-59191-0;SUBJMETA

30. Parvaiz MR, Mohanty S, Nayak SK, Mahanwar PA. Effect of surface modification of fly ash on the mechanical, thermal, electrical and morphological properties of polyetheretherketone composites. Mater Sci Eng A 2011;528:4277–86. https://doi.org/10.1016/J.MSEA.2011.01.026

31. Thomason JL. The influence of fibre length, diameter and concentration on the modulus of glass fibre reinforced polyamide 6,6. Compos Part A Appl Sci Manuf 2008;39:1732–8. https://doi.org/10.1016/J.COMPOSITESA.2008.08.001

32. Pal T, Pramanik S, Verma KD, Naqvi SZ, Manna PK, Kar KK. Fly ash-reinforced polypropylene composites. Handb Fly Ash 2021:243–70. https://doi.org/10.1016/B978-0-12-817686-3.00021-9

33. Hiremath P, Shettar M, Shankar MCG, Mohan NS. Investigation on effect of egg shell powder on mechanical properties of GFRP composites. Mater Today Proc 2018;5:3014–8. https://doi.org/10.1016/J.MATPR.2018.01.101

34. Fu SY, Feng XQ, Lauke B, Mai YW. Effects of particle size, particle/matrix interface adhesion and particle loading on mechanical properties of particulate–polymer composites. Compos Part B Eng 2008;39:933–61. https://doi.org/10.1016/J.COMPOSITESB.2008.01.002

35. Panda BP, Mohanty S, Nayak SK. Mechanism of Toughening in Rubber Toughened Polyolefin—A Review. Polym Plast Technol Eng 2015;54:462–73. https://doi.org/10.1080/03602559.2014.958777

36. Liang JZ, Li RKY. Rubber toughening in polypropylene: A review. J Appl Polym Sci 2000;77:409–17. https://doi.org/10.1002/(SICI)1097-4628(20000711)77:2

37. Ndiaye D, Matuana LM, Morlat-Therias S, Vidal L, Tidjani A, Gardette JL. Thermal and mechanical properties of polypropylene/wood-flour composites. J Appl Polym Sci 2011;119:3321–8. https://doi.org/10.1002/APP.32985

38. Fazli A, Rodrigue D. Effect of ground tire rubber (GTR) particle size and content on the morphological and mechanical properties of recycled high-density polyethylene (rHDPE)/GTR blends. Recycl 2021;6:44. https://doi.org/10.3390/RECYCLING6030044

39. Bouafif H, Koubaa A, Perré P, Cloutier A. Effects of fiber characteristics on the physical and mechanical properties of wood plastic composites. Compos Part A Appl Sci Manuf 2009;40:1975–81. https://doi.org/10.1016/J.COMPOSITESA.2009.06.003

40. Yao ZT, Chen T, Li HY, Xia MS, Ye Y, Zheng H. Mechanical and thermal properties of polypropylene (PP) composites filled with modified shell waste. J Hazard Mater 2013;262:212–7. https://doi.org/10.1016/J.JHAZMAT.2013.08.062

41. Xu B, Lin Z, Xian J, Huo Z, Cao L, Wang Y, et al. Preparation and characterization of polypropylene composites with nonmetallic materials recycled from printed circuit boards. J Thermoplast Compos Mater 2016;29:48–57. https://doi.org/10.1177/0892705713518788

42. Tucker JD, Lee S, Einsporn RL. A study of the effect of PP-g-MA and SEBS-g-MA on the mechanical and morphological properties of polypropylene/nylon 6 blends. Polym Eng Sci 2000;40:2577–89. https://doi.org/10.1002/PEN.11388